

# Harmonic Resonance Mode Analysis in $dq$ Domain

Abel A. Taffese<sup>1</sup>, Elisabetta Tedeschi<sup>2</sup>

Department of Electric Power Engineering  
Norwegian University of Science of Technology  
Trondheim, Norway

Email: abel.taffese@ntnu.no<sup>1</sup>, elisabetta.tedeschi@ntnu.no<sup>2</sup>

**Abstract**—Harmonic Resonance Mode Analysis (HRMA) is a technique developed to study harmonic resonance in a power system. Compared to conventional resonance analysis techniques, HRMA is a powerful method that can indicate the origin and the locations most affected by a given mode of resonance. The method has been shown to be effective for large scale resonance studies. However, very simplified models are used for representing power converters. With the proliferation of power converter interfaced energy sources in the future power system, there is a need to correctly model power converters in such studies. The main challenge is to correctly represent the control loops. The controllers are mostly designed in  $dq$  domain while the study is performed in phase domain. To address this problem, this paper proposes extension of HRMA to  $dq$  domain. Formulation of the problem in  $dq$  domain is presented in detail followed by verification using simple test cases. A detailed model of a voltage source converter for the aforementioned analysis is also developed and analysed using the test cases.

**Index Terms**—Harmonic Resonance Mode Analysis, HRMA, Resonance,  $dq$ , VSC.

## I. INTRODUCTION

Harmonics are undesired frequency components which pollute voltage and current of a power system. They might cause excessive voltage or current if their frequency aligns with the resonance frequencies of a system [1]. Resonance analysis is performed in order to prevent or mitigate such problems. The most common techniques for resonance analysis are frequency scan and Harmonic Resonance Mode Analysis (HRMA) [2]. Among them HRMA [3] gives powerful insight into resonance behaviour of a network. It can indicate the origin of a given resonance mode. Furthermore, using the sensitivity analysis [4], [5], mitigation action such as filter design can be carried out [6]. HRMA has been shown to be suitable for both small and large power systems [3]. It has also been used to analyse wind farms that include voltage source converters [7]. Because of the expected presence of such converters in future power systems [8], their correct modelling is critical for accurate results. The main challenge is the representation of the control loops. The controller are usually in  $dq$  domain [9] while HRMA is formulated in phase domain. Existing works [7] adopted Proportional Resonant (PR) controllers because they are easier to represent in phase domain. A better way to model the controllers is to do so in  $dq$  domain because they are naturally developed in this domain. This paper proposes an extension of the HRMA to  $dq$  domain. This approach can simply model a converter controlled in  $dq$  domain without making unnecessary simplifying assumptions.

The remainder of the paper is organized as follows. Section II deals with the formulation of HRMA in  $dq$  domain followed by component models in Section III. This is followed by verification using a simple test case. Then modelling of voltage source converter is presented in Sec-

tion V. This is followed by analysis including a voltage source converter. Limitations of the method are discussed in Section VII.

The following conventions definitions are used in this paper.

- Boldface small letters are used to denote column vectors while boldface capital letters are for matrices.
- $\mathbf{I}$  and  $\mathbf{J}$  matrices are defined as shown in (1).

$$\mathbf{I} = \begin{bmatrix} 1 & 0 \\ 0 & 1 \end{bmatrix} \quad \text{and} \quad \mathbf{J} = \begin{bmatrix} 0 & -1 \\ 1 & 0 \end{bmatrix} \quad (1)$$

where  $\mathbf{I}$  is the identity matrix and  $\mathbf{J}$  is a matrix that rotates its input by  $90^\circ$ .

- A quantity written in  $dq$  domain, e.g.  $x^{dq}$ , is a column vector whose first element is its  $d$ -axis component.
- Per unit (pu) values are defined as per [10]. In addition, since the resonance frequencies are read in per unit, all quantities in the system, including time, should be in per unit. The base value for time is the inverse of the frequency base,  $\omega_b$ .

## II. HRMA IN $dq$ DOMAIN

Formulation of HRMA in  $dq$  domain closely follows the formulation using real admittance matrix presented in [3], [11]. Assuming a symmetric and balanced operation, the voltage and current space phasors [12] can be written in complex form as shown in (2). The  $d$  and  $q$  axis components are real and imaginary components, respectively. The admittance matrix is also split into real and imaginary components, (3).

$$\mathbf{v}_{dq} = \mathbf{v}_d + j\mathbf{v}_q \quad \text{and} \quad \mathbf{i}_{dq} = \mathbf{i}_d + j\mathbf{i}_q \quad (2)$$

$$\mathbf{Y} = \mathbf{Y}_d + j\mathbf{Y}_q \quad (3)$$

The  $d$  and  $q$  axis components in (2) can be stacked to form column vectors, (4), to avoid the complex notation. Such an arrangement results in the admittance matrix of (5). The matrix has an identical structure to the real admittance matrix described in [3].

$$\mathbf{v}_{dq} = \begin{bmatrix} \mathbf{v}_d \\ \mathbf{v}_q \end{bmatrix} \quad \text{and} \quad \mathbf{i}_{dq} = \begin{bmatrix} \mathbf{i}_d \\ \mathbf{i}_q \end{bmatrix} \quad (4)$$

$$\mathbf{i}_{dq} = \begin{bmatrix} \mathbf{Y}_d & -\mathbf{Y}_q \\ \mathbf{Y}_q & \mathbf{Y}_d \end{bmatrix} \mathbf{v}_{dq} \quad (5)$$

Eigenvalues and eigenvectors of the matrix in (5) are given in (6) and (7), respectively [3].

$$\mathbf{\Lambda}_{dq} = \begin{bmatrix} \mathbf{\Lambda} & \mathbf{0} \\ \mathbf{0} & \mathbf{\Lambda}^* \end{bmatrix} \quad (6)$$

$$\mathbf{R}_{dq} = \frac{1}{\sqrt{2}} \begin{bmatrix} \mathbf{R} & \mathbf{R}^* \\ -j\mathbf{R} & j\mathbf{R}^* \end{bmatrix} \quad \mathbf{L}_{dq} = \frac{1}{\sqrt{2}} \begin{bmatrix} \mathbf{L} & j\mathbf{L} \\ \mathbf{L}^* & -j\mathbf{L}^* \end{bmatrix} \quad (7)$$

where  $\Lambda$  and  $\Lambda_{dq}$  are eigenvalues of the original and  $dq$  domain admittance matrices, respectively.  $\mathbf{R}_{dq}$  and  $\mathbf{L}_{dq}$  are right and left eigenvector matrices of the  $dq$  admittance matrix, respectively.  $\mathbf{R}$  and  $\mathbf{L}$  are right and left eigenvector matrices of the original matrix. The asterisk represents complex conjugate operator. Participation factors are calculated by using (8) where  $\mathbf{r}_i$  and  $\mathbf{l}_i$  are right and left eigenvectors of the  $i^{\text{th}}$  mode, respectively.

$$\mathbf{P}\mathbf{f}_i = \text{diag}(\mathbf{r}_i \times \mathbf{l}_i) \quad (8)$$

From these results, the following points can be noted.

- There is a functionality equivalence between the  $dq$  formulation and the original one, proposed in [3], due to the fact that they both contain the same information.
- All the modes of the original system are present in the  $dq$  domain with additional complex conjugate duplicates.
- Since both the left and right eigenvectors are scaled by  $\sqrt{2}$  in (7), participation factors of the  $d$  and  $q$  axis buses will be half of those of the original system.

The admittance matrix is built by interconnecting components as per the circuit under consideration. However, as will be shown in the next section, the peculiarity in the  $dq$  case is that each component is represented by a  $2 \times 2$  matrix. This is shown in (9) where  $\mathbf{Y}_c$  is the component admittance matrix.

$$\mathbf{Y}_c = \begin{bmatrix} y_{dd} & y_{dq} \\ y_{qd} & y_{qq} \end{bmatrix} \quad (9)$$

$$\mathbf{Y}_{sys} = \begin{bmatrix} \mathbf{Y}_{dd} & \mathbf{Y}_{dq} \\ \mathbf{Y}_{qd} & \mathbf{Y}_{qq} \end{bmatrix} \quad (10)$$

The system node admittance matrix,  $\mathbf{Y}_{sys}$  in (10), can be built as a block matrix with components  $\mathbf{Y}_{dd}$ ,  $\mathbf{Y}_{dq}$ ,  $\mathbf{Y}_{qd}$ , and  $\mathbf{Y}_{qq}$ . Each block is built using standard method [13] applied on the circuit with the branch elements replaced by a corresponding element in the component admittance matrix,  $\mathbf{Y}_c$ . For instance,  $\mathbf{Y}_{dd}$  is built by using the standard method on the circuit with all the branch elements replaced by a conductance equal to the  $y_{dd}$  element of the same branch. The next section deals with modelling of basic components in  $dq$  domain.

### III. MODELLING OF BASIC COMPONENTS

In order to perform HRMA in  $dq$  domain, component models [14] should first be transformed to  $dq$  domain. The following sections present modelling of the basic building blocks in a system.

#### A. Capacitor

Dynamics of a capacitor, in phase domain, is governed by the differential equation relating the voltage across it with the current flowing through it, (11).

$$C \frac{d\mathbf{v}_c^{abc}}{dt} = \mathbf{i}_c^{abc} \quad (11)$$

Where  $C$  is the per phase capacitance. Transforming (11) in to  $dq$ , at the nominal grid frequency of  $\omega_g$  pu, gives (12).

$$C \frac{d\mathbf{v}_c^{dq}}{dt} + \omega_g C \mathbf{J} \mathbf{v}_c^{dq} = \mathbf{i}_c^{dq} \quad (12)$$

Applying Laplace transform to (12) results in

$$(sC\mathbf{I} + \omega_g C \mathbf{J}) \mathbf{v}_c^{dq} = \mathbf{i}_c^{dq} \quad (13)$$

Where  $s$  is the Laplace variable. Frequency response is obtained by replacing  $s$  with  $jh$ , where  $h$  is the per unit harmonic frequency and  $j$  is the complex operator. Multiplication by  $j$  results in a  $90^\circ$  rotation in the complex plane, similar to  $J$  in (1). Taking these facts into consideration, the final frequency domain equation is given by (14).

$$(h + \omega_g) \mathbf{J} \mathbf{v}_c^{dq} = \mathbf{i}_c^{dq} \quad (14)$$

Since the grid frequency, and hence the transformation frequency, is equal to 1 pu, the admittance associated with a capacitor in  $dq$  domain is given by (15). A point to note from (14) is that the transformation results in a left shift in frequency by 1, i.e. the second harmonic in  $abc$  domain would give a first harmonic in  $dq$  domain. This fact should be considered when reading resonance frequencies.

$$\mathbf{Y}_c = (h + 1) C \mathbf{J} \quad (15)$$

The admittance matrix,  $\mathbf{Y}_c$ , is a  $2 \times 2$  matrix where the diagonals are  $d$  and  $q$  bus admittances and the off-diagonals are cross-coupling terms.

#### B. Inductor

Following a similar reasoning, the admittance matrix for an inductor, including coil resistance, is given by (16) where  $R_L$  and  $L$  are resistance and inductance values of the inductor, respectively.

$$\mathbf{Y}_l = \frac{-1}{\sqrt{R_L^2 + ((h + 1)L)^2}} (R_L \mathbf{I} + (h + 1) L \mathbf{J}) \quad (16)$$

A special case of a pure inductance can be obtained by setting  $R_L = 0$  in (16).

#### C. Resistor

A resistor is the simplest component since it does not involve differential equations. Its admittance is given by (17) where  $R$  is the resistance value.

$$\mathbf{Y}_r = \frac{1}{R} \mathbf{I} \quad (17)$$

More complicated components such as cables can be built as interconnection of the basic components described in this section.

### IV. A SIMPLE TEST CASE

A simple test case [3] is presented in this section in order to validate the proposed method. The circuit is shown in Fig. 1. Two critical modes were identified in [3]; one at 9.62 and the other at 51.6 pu. Modal scan using the original method [3] results in Fig. 2 where the two modes, 2 and 3, can clearly be identified. Participation factors, computed using (8), are presented in Table I. These values are in close agreement with the ones presented in [3].

A corresponding modal scan using the proposed  $dq$  method is presented in Fig. 3 where the number of modes has doubled as expected. Three of these modes,  $d$ -axis, are identical to the remaining three,  $q$ -axis. Four resonant modes can be identified at 8.62 and 50.61. These frequencies are less than the original results by 1. As discussed earlier, the transformation to  $dq$  domain is the source of this difference.

Participation factors computed for the  $dq$  case are displayed in Table II. The values are half of the original ones as was stated in Section II. These results have successfully

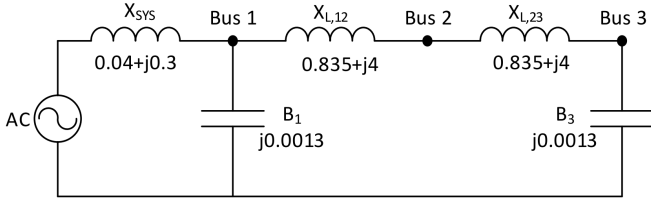


Fig. 1: Circuit of the three bus case [7]

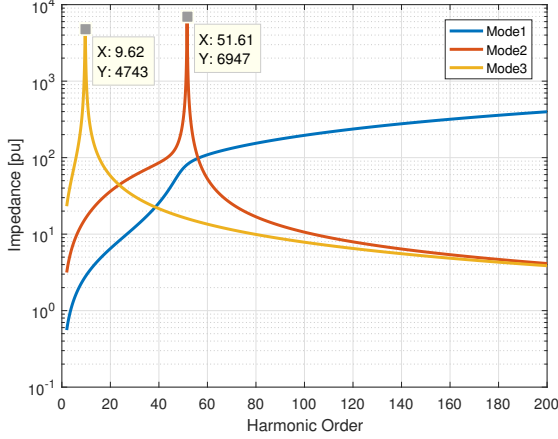


Fig. 2: Resonant modes in the three bus case using the original method.

TABLE I: Participation factors for the three bus case

Bus	Mode 2 (51.61pu)	Mode 3 (9.62pu)
Bus1	<b>0.8109</b>	0.0011
Bus2	0.1880	0.2118
Bus3	0.0011	<b>0.7871</b>

TABLE II: Participation factors for the three bus case

Bus	Mode 3	Mode 4	Mode 5	Mode 6
Bus1, d	<b>0.4054</b>	<b>0.4054</b>	0.0006	0.0006
Bus2, d	0.0940	0.0940	0.1059	0.1059
Bus3, d	0.0006	0.0006	<b>0.3936</b>	<b>0.3936</b>
Bus1, q	<b>0.4054</b>	<b>0.4054</b>	0.0006	0.0006
Bus2, q	0.0940	0.0940	0.1059	0.1059
Bus3, q	0.0006	0.0006	<b>0.3936</b>	<b>0.3936</b>

validated the proposed method against the one proposed in [3]. The next section introduces extension to modelling of a voltage source converter.

## V. MODELLING OF A VOLTAGE SOURCE CONVERTER

Circuit of a voltage source converter is depicted in Fig. 4. For the sake of simplicity L-C filter is assumed. A state-space modelling approach is followed in this section.

### A. Converter Dynamics

The current flowing in to the converter is governed by (18).

$$L_c \frac{d\mathbf{i}_{c,dq}}{dt} = \mathbf{v}_{p,dq} - (R_c \mathbf{I} + \omega_g L_c \mathbf{J}) \mathbf{i}_{c,dq} - \mathbf{v}_{c,dq} \quad (18)$$

The parameters can be read from Fig. 4.  $\omega_g$  is the grid frequency in pu, normally set equal to 1. The converter output  $\mathbf{v}_{c,dq}$  is equal to the output of the current controllers in pu, Fig. 5. This is also shown in (19) where  $L_{ff}$  is a feed-forward decoupling terms.  $\mathbf{y}_{pi,dq}$  is the output of the two PI controllers. Setting  $L_{ff} = L_c$  results in perfect decoupling of the  $d$  and  $q$  axes. However, this is rarely achievable

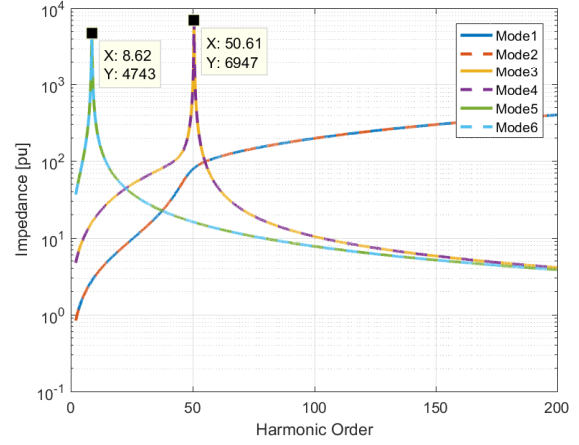


Fig. 3: Resonant modes in the three bus case using the proposed method.

in practice. Therefore,  $L_{ff} = (1 + 0.2) L_c$  is used in this analysis to account for decoupler mismatch.

$$\mathbf{v}_{c,dq} = \mathbf{v}_{p,dq} - \omega_g L_{ff} \mathbf{J} \mathbf{i}_{c,dq} - \mathbf{y}_{pi,dq} \quad (19)$$

The PI current controllers are modelled by (20) and (21) where  $\mathbf{x}_{dq}$  is a vector containing integral states of the controller.

$$\frac{d\mathbf{x}_{dq}}{dt} = \frac{1}{\omega_b} (-\mathbf{i}_{c,dq} + \mathbf{i}_{dq}^*) \quad (20)$$

$$\mathbf{y}_{pi,dq} = k_p (-\mathbf{i}_{c,dq} + \mathbf{i}_{dq}^*) + k_i \mathbf{x}_{dq} \quad (21)$$

$k_p$  and  $k_i$  are proportional and integral gains of the controllers, respectively.  $\mathbf{i}_{dq}^*$  is the current reference possibly coming from outer controllers. Such controllers can be implemented in different ways for different applications. In most cases they control active and reactive powers using standard PI controllers. Consequently, the converter acts like a constant power load which is undesirable because it reduces damping in a system. To overcome this challenge, droop action is often included pushing the behaviour towards passive impedance. If the control bandwidth is high enough, in the order of few  $kHz$  as is the case in active power filters, the converter can emulate a passive element over a wide frequency range. The next section deals with incorporation of this kind of behaviour in the proposed method. Although this operation is an oversimplification of the real controller, it can be a good illustrative example to show simplicity and effectiveness of the proposed method in modelling different controllers.

### B. Inductive and Resistive Outer Control

When the outer controller is behaving as an inductor over the desired frequency range, the current references are governed by (22).

$$L_e \frac{d\mathbf{i}_{L,dq}^*}{dt} = -\omega_g L_e \mathbf{J} \mathbf{i}_{L,dq}^* + \mathbf{v}_{p,dq} \quad (22)$$

where  $\mathbf{i}_{L,dq}^*$  is the current reference generated by an inductive outer control.  $L_e$  is the emulated inductance value. Resistive behaviour is implemented as shown (23).  $R_e$  is the emulated resistance value. If a parallel R-L behaviour is desired, the two outputs,  $\mathbf{i}_{L,dq}^*$  and  $\mathbf{i}_{R,dq}^*$ , should be added together.

$$\mathbf{i}_{R,dq}^* = \frac{1}{R_e} \mathbf{v}_{p,dq} \quad (23)$$

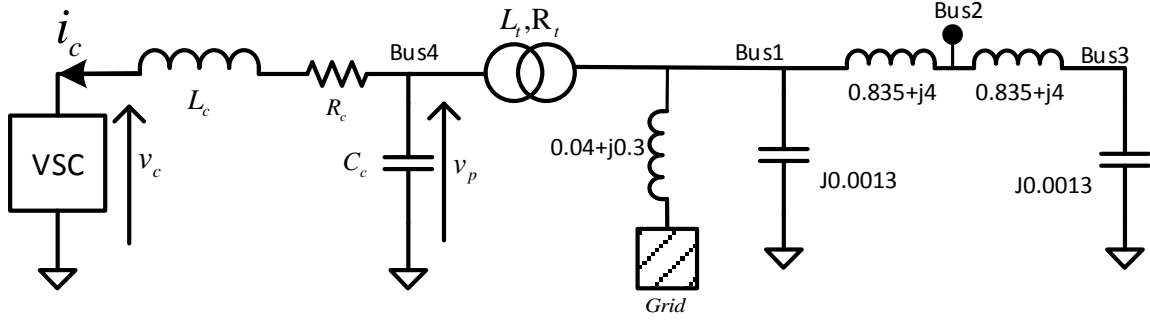


Fig. 4: Voltage source converter test circuit.

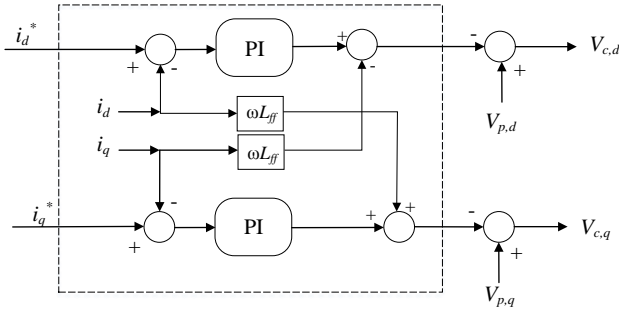


Fig. 5: dq current control scheme.

Eqs. (24) and (25) give the complete state-space description of the converter. The  $\mathbf{D}$  matrix is  $\mathbf{0}$  since there is no input feed-through.  $\mathbf{x}$  is a column vector containing all the states and  $\mathbf{x}_{dq}$  contains states of the two controllers (d and q-axis).

$$\mathbf{x} = \begin{bmatrix} \mathbf{i}_{c,dq} \\ \mathbf{x}_{dq} \\ \mathbf{i}_{L,dq}^* \end{bmatrix} \quad \mathbf{A} = \begin{bmatrix} \frac{1}{L_c} \mathbf{a}_{11} & \frac{k_i}{L_c} \mathbf{I} & \frac{k_p}{L_c} \mathbf{I} \\ -\frac{1}{\omega_b} \mathbf{I} & \mathbf{0} & \frac{1}{\omega_b} \mathbf{I} \\ \mathbf{0} & \mathbf{0} & -\omega_g \mathbf{J} \end{bmatrix} \quad (24)$$

$$\mathbf{a}_{11} = -((k_p + R_c) \mathbf{I} + \omega_g (L_c - L_{ff}) \mathbf{J})$$

$$\mathbf{B} = \begin{bmatrix} \left( \frac{1 + R_e}{R_e L_c} \right) \mathbf{I} \\ \frac{1}{\omega_b R_e} \mathbf{I} \\ \frac{1}{L_e} \mathbf{I} \end{bmatrix} \quad \mathbf{C} = [\mathbf{I} \quad \mathbf{0} \quad \mathbf{0}] \quad (25)$$

Now the next step is to convert these equations to frequency domain. This is done as shown in (26). The matrix  $\mathbf{J}_b$  is a rotation matrix similar to the one discussed in Section III. Its purpose is to avoid the complex frequency  $s$  from the transfer functions.

$$\mathbf{Y}_{VSC} = \mathbf{C} (h\mathbf{J}_b - \mathbf{A})^{-1} \mathbf{B} \quad (26)$$

$$\mathbf{J}_b = \begin{bmatrix} \mathbf{J} & \mathbf{0} & \mathbf{0} \\ \mathbf{0} & \mathbf{J} & \mathbf{0} \\ \mathbf{0} & \mathbf{0} & \mathbf{J} \end{bmatrix}$$

TABLE III: Converter parameters

Parameter Name	Value
Per unit filter inductance, $L_c$	0.1
Per unit filter resistance, $R_c$	0.01
Per unit filter capacitance, $C_c$	0.044
Per unit transformer inductance, $L_t$	0.1
Per unit transformer resistance, $R_t$	0.01
Current controller proportional gain, $k_p$	24
Current controller integral gain, $k_i$	628
Feed-forward decoupling inductance, $L_{ff}$	$1.2 \cdot L_c$
Base frequency in rad/s, $\omega_b$	$2\pi \cdot 50$
Per unit emulated inductance, $L_e$	2
Per unit emulated resistance, $R_e$	2

## VI. CASE STUDY WITH THE CONVERTER CONNECTED

In this section, connection of a voltage source converter, with parameters given in Table III, to the three bus circuit of Fig. 1 is analysed. Subsequent sections present analysis of the following three cases:

- Case 1: Only Passive elements, transformer and filter capacitor, connected.
- Case 2: Converter and passive elements connected with the converter operating in pure inductive mode,  $L_e = 2pu$ .
- Case 3: Converter and passive elements connected with the converter operating in L-R mode,  $L_e = 2pu$  and  $R_e = 2pu$ .

### A. Case 1

In case 1 the passive elements of the converter are connected to the three bus circuit. This is expected to shift the resonance frequencies in the circuit. The result of modal sweep on this case is shown in Fig. 6. Three resonant modes can be identified from the figure. The corresponding participation factors are displayed in Table IV where the duplicate modes are not included to save space. It can be seen that *Mode 7* is the new mode introduced by connection of the converter. This mode is strongly related to *Buses 2 and 3* with a small contribution from the other buses. The remaining modes have only undergone a frequency shift from the original circuit, Fig. 3.

### B. Case 2

In the second case, the converter is connected and emulates a pure inductive behaviour. The result is shown in Fig. 7. It should be noted that *Mode 7* in this case is the same as *Mode 5* in Case 1. The order is reversed because the eigenvalues values are sorted in increasing order.

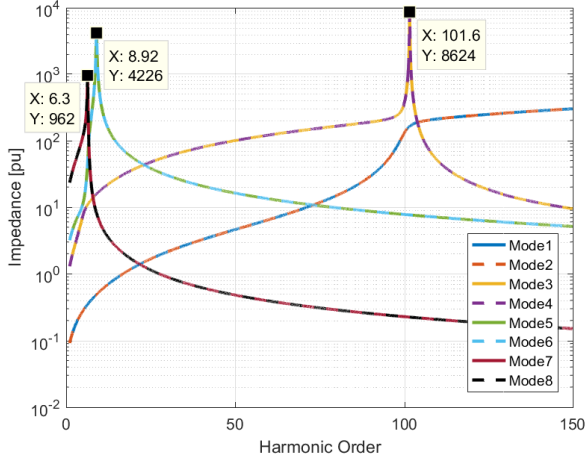


Fig. 6: Resonant Modes for Case 1. Only Passive elements, transformer and filter capacitor, connected.

TABLE IV: Participation factors for Case 1

Bus	Mode 3 (101.6pu)	Mode 5 (8.92pu)	Mode 7 (6.3pu)
<i>Bus1, d</i>	<b>0.4010</b>	0.0003	0.0469
<i>Bus2, d</i>	0.0988	0.0953	0.1268
<i>Bus3, d</i>	0.0000	<b>0.4034</b>	<b>0.2458</b>
<i>Bus4, d</i>	0.0002	0.0010	0.0805
<i>Bus1, q</i>	<b>0.4010</b>	0.0003	0.0469
<i>Bus2, q</i>	0.0988	0.0953	0.1268
<i>Bus3, q</i>	0.0000	<b>0.4034</b>	<b>0.2458</b>
<i>Bus4, q</i>	0.0002	0.0010	0.0805

From Table V, it can be observed that *Bus 4* has taken the dominance over the mode at 7.21pu. This is due to the resonance between the filter capacitance,  $C_c$ , and the emulated inductance,  $L_e$ , under the influence of the other components.

### C. Case 3

A resistive behaviour is added in Case 3 to investigate the impact of adding damping to *Bus 4*. Figure 8 shows the resulting plot. It can clearly be seen that the resistive behaviour improved damping of the mode at 7.33; the peak decreased from  $\approx 55$  to  $\approx 30$ pu. However, the same action results in a decrease in damping of the mode at 8.97. The participation factors, Table VI, convey similar information to those of Case 2.

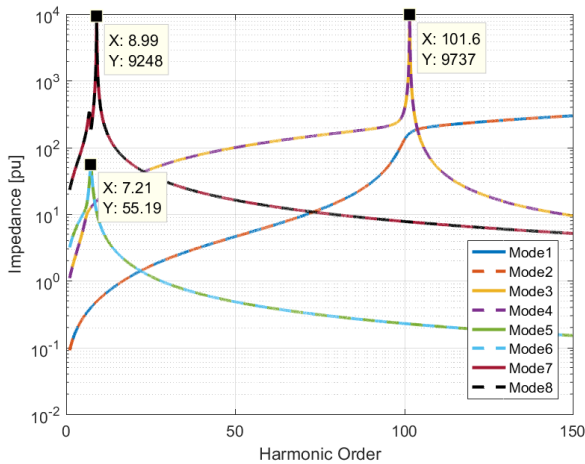


Fig. 7: Resonant Modes for Case 2.

TABLE V: Participation factors for Case 2: Converter and passive elements connected with the converter operating in pure inductive mode,  $L_e = 2pu$ .

Bus	Mode 3 (101.6pu)	Mode 5 (7.21pu)	Mode 7 (8.99pu)
<i>Bus1, d</i>	<b>0.4014</b>	0.1416	0.0006
<i>Bus2, d</i>	0.0983	0.0434	0.0937
<i>Bus3, d</i>	0.0000	0.0608	<b>0.4041</b>
<i>Bus4, d</i>	0.0002	<b>0.2542</b>	0.0017
<i>Bus1, q</i>	<b>0.4014</b>	0.1416	0.0006
<i>Bus2, q</i>	0.0983	0.0434	0.0937
<i>Bus3, q</i>	0.0000	0.0608	<b>0.4041</b>
<i>Bus4, q</i>	0.0002	<b>0.2542</b>	0.0017

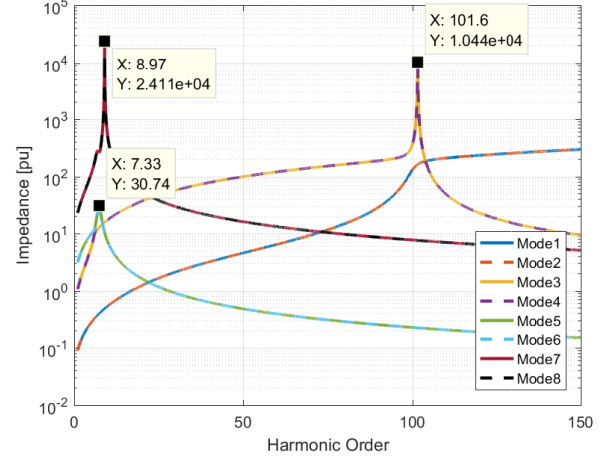


Fig. 8: Resonant modes for Case 3: Converter and passive elements connected with the converter operating in L-R mode,  $L_e = 2pu$  and  $R_e = 2pu$ .

Figure 9 shows the result of Case 3 with perfect decoupling in the controller. The resonance is now slightly better damped and the frequencies have shifted marginally. The change is not significant for this specific case. However, the main point is that the proposed method allows modelling of controller details that might not be accessible in phase domain.

## VII. LIMITATIONS OF THE METHOD

The proposed method, as formulated so far, has the following limitations:

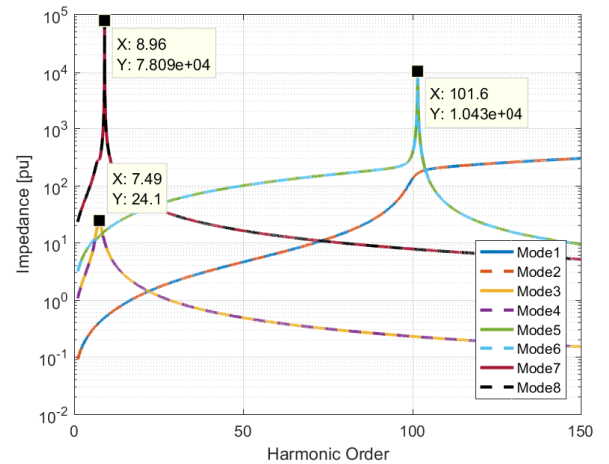


Fig. 9: Resonant modes for Case 3 with  $L_{ff} = L_c$

TABLE VI: Participation factors for Case 3

Bus	Mode 3 (101.6pu)	Mode 5 (7.33pu)	Mode 7 (8.97pu)
<i>Bus1, d</i>	<b>0.4014</b>	0.1618	0.0006
<i>Bus2, d</i>	0.0984	0.0286	0.0941
<i>Bus3, d</i>	0.0000	0.0188	<b>0.4037</b>
<i>Bus4, d</i>	0.0002	<b>0.2909</b>	0.0016
<i>Bus1, q</i>	<b>0.4014</b>	0.1618	0.0006
<i>Bus2, q</i>	0.0984	0.0286	0.0941
<i>Bus3, q</i>	0.0000	0.0188	<b>0.4037</b>
<i>Bus4, q</i>	0.0002	<b>0.2909</b>	0.0016

- It does not allow different parameter values for the d and q axes, for instance, controller parameters. If this is violated, the problem will be different from the real admittance matrix form (5). Therefore, a different approach should be followed.
- In the case of non symmetric or unbalanced operations, there will be negative and zero sequence component which are transformed in to *dq* causing frequency overlap. Due to this fact the method fails to give accurate results.

In most cases, both limitations can be avoided by making reasonable assumptions of symmetric and balanced three phase system. However, further development is needed to make the approach applicable to a wider range of cases which are not readily compatible with the current formulation.

### VIII. CONCLUSION

This paper proposed a method to perform HRMA in *dq* domain. This was motivated by the fact that most voltage source converter are controlled in *dq* domain. The detailed derivation showed that the method gives similar results to the original HRMA technique. This was also supported by analysis performed in the three bus case. Further, a detailed model of a voltage source converter was presented. This was then used to demonstrate different converter control

[8] M. Molinas, "The role of power electronics in distributed energy systems," in *Proceedings of the 5th AIST Symposium on Distributed Energy Systems*, 2008.

behaviours and their impact on resonance. The method, as presented in this paper, is limited to symmetric and balanced systems. It does not allow different parameters in the d and q axes. Further development is required to make the method applicable to a general case.

### REFERENCES

- [1] S. Ranade and W. Xu, "An overview of harmonics modeling and simulation," *IEEE Task Force on Harmonics Modeling and Simulation*, p. 1, 2007.
- [2] K. M. Hasan, K. Rauma, P. Rodriguez, J. I. Candela, R. S. Muñoz-Aguilar, and A. Luna, "An overview of harmonic analysis and resonances of large wind power plant," in *IECON 2011-37th Annual Conference on IEEE Industrial Electronics Society*. IEEE, 2011, pp. 2467–2474.
- [3] W. Xu, Z. Huang, Y. Cui, and H. Wang, "Harmonic resonance mode analysis," *IEEE Transactions on Power Delivery*, vol. 20, no. 2, pp. 1182–1190, Apr. 2005.
- [4] Y. Cui and X. Wang, "Modal frequency sensitivity for power system harmonic resonance analysis," *IEEE Transactions on Power Delivery*, vol. 27, no. 2, pp. 1010–1017, 2012.
- [5] Z. Huang, Y. Cui, and W. Xu, "Application of modal sensitivity for power system harmonic resonance analysis," *IEEE Transactions on Power Systems*, vol. 22, no. 1, pp. 222–231, 2007.
- [6] M. Esmaili, H. A. Shayanfar, and A. Jalilian, "Modal analysis of power systems to mitigate harmonic resonance considering load models," *Energy*, vol. 33, no. 9, pp. 1361–1368, 2008.
- [7] H. A. Brantsæter, "Harmonic resonance mode analysis and application for offshore wind power plants," Master's thesis, Norwegian University of Science and Technology, Dec. 2015.
- [9] B. Bahrani, A. Karimi, B. Rey, and A. Rufer, "Decoupled dq-current control of grid-tied voltage source converters using nonparametric models," *IEEE Transactions on Industrial Electronics*, vol. 60, no. 4, pp. 1356–1366, 2013.
- [10] P. Kundur, N. J. Balu, and M. G. Lauby, *Power system stability and control*. McGraw-hill New York, 1994, vol. 7.
- [11] Y. Cui and W. Xu, "Harmonic resonance mode analysis using real symmetrical nodal matrices," *IEEE Transactions on Power Delivery*, vol. 22, no. 3, pp. 1989–1990, Jul. 2007.
- [12] N. Mohan, *Advanced Electric Drives: Analysis, Control, and Modeling Using MATLAB / Simulink*. Wiley, 2014. [Online]. Available: <https://books.google.no/books?id=PaULBAAQBAJ>
- [13] J. J. Grainger and W. D. Stevenson, *Power system analysis*. McGraw-Hill, 1994.
- [14] W. Xu, "Component modeling issues for power quality assessment," *IEEE Power Engineering Review*, vol. 21, no. 11, pp. 12–17, 2001.